PROCEEDINGS, Fourtieth Workshop on Geothermal Reservoir Engineering
Stanford University, Stanford, California, January 26-28, 2015
SGP-TR-204

Assessing Fracture Connectivity using Stable and Clumped Isotope Geochemistry of Calcite Cements

Kristina K. Sumner[1], Erin R. Camp[2], Katharine W. Huntington[1], Trenton C. Cladouhos[3], Matt Uddenberg[3]

[1]University of Washington, Box 351310, Seattle, WA 98195-1310

[2]Department of Earth and Atmospheric Sciences, Cornell University, Ithaca, NY 14853

[3]AltaRock Energy, Inc., 4010 Stone Way N., Suite 400, Seattle, WA 98103

E-mail: kksumner@u.washington.edu

Keywords: Stable Isotopes, Clumped Isotope Thermometry, Geochemistry, Cathodoluminescence Microscopy, Flow Path Connectivity, Fracture Connectivity

ABSTRACT

Understanding flow path connectivity within a geothermal reservoir is a critical component for efficiently producing sustained flow rates of hot fluids from the subsurface. We present a new approach for characterizing subsurface fracture connectivity that uses clumped isotope (Δ_{47}) thermometry along with stable isotope analysis ($\delta^{18}O$ and $\delta^{13}C$) and cold cathodoluminescence (CL) microscopy of fracture-filling calcite cements from a geothermal reservoir in northern Nevada. Calcite cement samples were derived from both drill cuttings and core samples taken at various depths from wells within the geothermal field. CL microscopy of some fracture filling cements shows banding parallel to the fracture walls as well as brecciation, indicating that the cements are related to fracture opening and fault slip. Variations in trace element composition indicated by the luminescence patterns reflect variations in the composition and source of fluids moving through the fractures as they opened episodically. Calcite $\delta^{13}C$ and $\delta^{18}O$ results also show significant variation among the sampled cements, reflecting multiple generations of fluids and fracture connectivity. Clumped isotope analyses performed on a subset of the cements analyzed for conventional $\delta^{18}O$ and $\delta^{13}C$ mostly show calcite growth temperatures around 150°C, which indicates a common temperature trend for the geothermal reservoir. However, calcite cements sampled along faults located within the well field showed both cold (19°C) and hot (226°C) temperatures. The anomalously cool temperature found along the fault, using estimates from clumped isotope thermometry, suggests a possible connection to surface waters for the geothermal source fluids for this system. This information may indicate that some of the faults within the well field are transporting meteoric water from the surface to be heated at depth, which then is circulated through a complex network of fractures and other faults.

1. INTRODUCTION

Geothermal fields are dynamic systems that are continually changing and evolving through time (Lowell *et al.*, 1993; Bruel, 2002; Yasuhara *et al.*, 2006). Because of the dynamic nature of these systems, regular evaluation and adjustments are essential for maximum energy extraction results. However, before field optimization can be achieved, an in-depth understanding of fluid pathways including fluid sources and recharge locations is essential (Horne and Rodriquiez, 1983; Sheridan *et al.*, 2003). This research investigates a new tool, clumped isotope geothermometry (Δ_{47}), along with stable isotope analyses of $\delta^{18}O$ and $\delta^{13}C$ and cold-cathodoluminescence (CL) to evaluate precipitated calcite cements deposited by geothermal fluids along the reservoir fracture network. Conventional oxygen and carbon isotopes (i.e., $\delta^{18}O$ and $\delta^{13}C$ values) can reflect fluid composition and source, and the addition of clumped isotope geothermometry (Δ_{47}) complements this data by independently recording past fluid temperatures (Bergman *et al.*, 2013). Prior stable and clumped isotope research along faults has shown promising results in the ability to determine the thermal evolution of these structures and their source fluids (Bergman *et al.*, 2013; Budd et al., 2013; Loyd et al., 2013; Swanson *et al.*, 2012). The results of this pilot study show how to apply and interpret conventional and clumped isotope data for geothermal reservoir calcite cements. Specifically, the potential of clumped isotope geothermometry to help assess fracture connectivity and geothermal reservoir characteristics in the past may benefit both geothermal resource managers and developers in future reservoir characterization and optimization of production and injection programs.

1.1 Geology

Blue Mountain is an eastward tilted fault block located within the Basin and Range Province in northern Nevada (Figure 1). Blue Mountain is positioned on the north-central end of the of the Luning-Fencemaker fold-and-thrust belt (Wyld, 2002). There are three predominant stratigraphic units of Triassic age found within this area, which are metamorphosed shales of phyllite and black slate, interbeds of metasandstone, and rare (3-4%) occurrences of limestone (Wyld, 2002). Deformation within these units shows two strain regimes that reflect northwest-southeast crustal shortening followed by low-grade metamorphism (phase 1), and minor northeast-southwest shortening (phase 2) (Wyld, 2002). Locally, within the Blue Mountain geothermal field, there are multiple fault zones located on the western, northwestern, and southwestern edges. These faults merge within the area of the geothermal field on the western flanks of Blue Mountain (Faulds and Melosh, 2008). The fault-controlled geothermal site has five production wells located in the center of the field with nine injectors along the perimeter, and four idle wells.

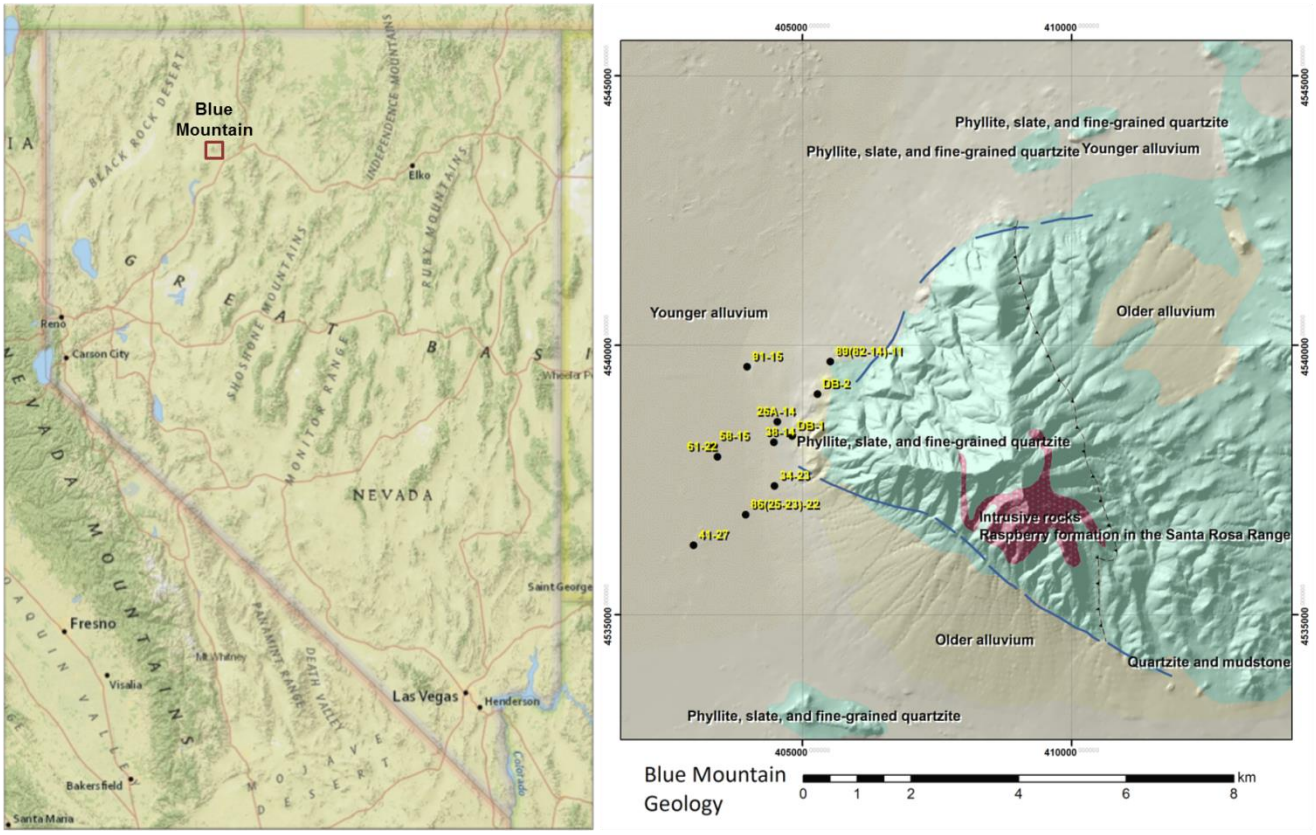

Figure 1: (Left) Location of Blue Mountain in the Basin and Range Province, Nevada. Left map courtesy of ArcMap™ software by Esri. (Right) Map of geothermal site located on the west flanks of Blue Mountain with local geology illustrated. Wells that were used in this study are labeled. Right image is courtesy of Mike Swyer and AltaRock Energy.

2. SAMPLING AND ANALYSES

For this investigation, calcite cements were derived from drill cuttings taken from nine wells (26A-14, 34-23, 38-14, 41-27, 58-15, 61-22, 86-22, 89-11, and 91-15) and from solid rock samples selected from two cores (DB-1 and DB-2), which are described by Ponce *et al.* (2009). Samples were taken from various depths within each of the wells and were selected based on the prevalence of calcite reported in corresponding drill logs from Tecton Geologic, 2009. Additionally, calcite found adjacent to zones associated with drilling mud losses or fault gouge reported within the drill logs were also targeted for analyses. These features may indicate the presence of faults, and/or mark an area that a given well has intersected a fluid conduit.

2.1 Cold Cathodoluminescence (CL) Microscopy

High-polished thin sections, cut perpendicular to fracture plane, were created from seven core samples taken from both DB-1 and DB-2. A Technosyn Luminoscope was used for our analysis to characterize the carbonate cements in thin section. Cold cathodoluminescence microscopy shows changes in chemical composition by concentrating a stream of electrons on the sections (De Abajo, 2010). The bombardment of electrons either excites impurities, commonly Mn^{2+} and Fe^{2+}, within the calcite crystal lattice or the impurities absorb the induced energy stream (Boggs and Krinsley, 2006). Variations in concentration of Mn^{2+} and Fe^{2+} found within calcite cement are reflected as changes in the intensity and color observed during electron stimulation (Machel, 1985). Overall, color changes observed within a calcite sample correlate to changes in fluid composition, which may be observed as yellowish-orange to red with lighter or darker hues (Boggs and Krinsley, 2006).

2.2 Stable Isotope Analysis

Seventy-two calcite samples from eleven wells, which included both drill cuttings and core, were analyzed for their carbon and oxygen isotopic compositions (Table 1). For each given well and well depth, two separate samples of calcite were collected from the drill cuttings based on visual differences in the characteristics of the calcite pieces (i.e. color and texture). The carbonate samples (0.02 – 0.12 mg) taken from drill cuttings were pulverized using an agate mortar and pestle. The calcite taken from core samples was extracted using a rotary drill tool (i.e. Dremel tool). All seventy-two samples were then processed on a Kiel III carbonate device coupled to a Finnigan Delta Plus mass spectrometer. The measured $\delta^{18}O$ and $\delta^{13}C$ values are referenced to Vienna Peedee Belemnite (VPDB) (Slater *et al.*, 2001).

2.3 Clumped Isotope (Δ_{47}) Analysis

A subset of nineteen samples was selected for clumped isotope Δ_{47} analysis. The clumped isotope samples include fourteen samples from drill cuttings and five samples from core (Table 1). This subset was selected to span the range of $\delta^{18}O$ and $\delta^{13}C$ values observed in the conventional stable isotope dataset. The carbonate samples (8-12 mg) selected from drill cuttings were powdered using an agate mortar and pestle, and samples taken from core were extracted using a rotary drill tool. All nineteen samples were pre-treated using a 3 percent solution of hydrogen peroxide (H_2O_2) for 45 minutes to remove organic material (Bergman *et al.*, 2013). Following this procedure, the prepared samples were digested in a common phosphoric acid bath (H_2PO_4) held at 90 °C to produce CO_2, which then passed through multiple cryogenic traps and a poropac trap to purify the CO_2 sample (Passey *et al.*, 2012). The CO_2 gasses were analyzed using a mass spectrometer (Thermo MAT253) configured to measure masses 44-49 inclusive (Huntington *et al.*, 2009). Furthermore, the nineteen calcite cement samples that were selected for clumped isotope analysis require 8-12 mg of pure calcite per replicate. For nine of the nineteen samples, it was possible to obtain sufficient material for analysis from a single calcite vein generation. For the other ten samples, calcite from two smaller veins from the same well and depth was combined to obtain enough material. For these "combined" samples, conventional $\delta^{18}O$ and $\delta^{13}C$ analysis of the vein calcites was conducted to evaluate homogeneity of the sample. Two of the combined samples (4127-4700 and 8622-3610) were determined to be heterogeneous by these methods; the apparent clumped isotope temperatures for these two samples do not reflect actual temperatures of calcite formation from paleofluids, and are not considered further.

The Δ_{47} geothermometer is based on the tendency of heavy carbon and oxygen isotopes in calcium carbonate ($CaCO_3$) to preferentially "clump" together as a function of the temperature at which the calcite precipitated (Schauble *et al.*, 2006; Ghosh *et al.*, 2006; Eiler, 2007). These are known as isotopologues, which are molecules that have the same chemical composition, but differ in their isotopic composition (Eiler, 2007). The Δ_{47} values reported are given in the absolute reference frame, which is a standardized reference frame in which sample CO_2 isotopologue values are referenced to equivalent measured values of CO_2 equilibrated at known temperatures (ARF; Dennis *et al.*, 2011). The clumped isotope paleothermometer is unique in that it does not rely on the composition of the fluid from which the carbonate cement formed (Ghosh *et al.*, 2006). This feature is extremely important for our study, because the paleo-composition of the subsurface fluids within the Blue Mountain geothermal field is not independently known. Once the temperature and the $\delta^{18}O_{calcite}$ values are determined via laboratory analysis, the $\delta^{18}O_{H2O}$ value can be calculated (e.g., using the equation of Kim and O'Neil, 2007). All $\delta^{18}O_{H2O}$ values are referenced to Vienna Standard Mean Ocean Water (VSMOW).

Sample	# Replicates	$\delta^{13}C$ (‰),	$\delta^{13}C$ (‰),	$\delta^{18}O_{carb}$ (‰),	$\delta^{18}O_{carb}$ (‰),	$\delta^{18}O_{H2O}$ (‰),	$\delta^{18}O_{H2O}$ (‰),	Δ_{47} (‰)	Δ47 (‰)	Δ47 (‰)	T(Δ_{47}) (°C)	T(Δ_{47})
	n	(VPDB)	Stnd error	(VPDB)	Stnd error	(VSMOW)	Stnd error	ARF	Stnd Error	Stnd Dev	Passey & Henkes	Stnd error
26A14-1680-2	1	-8.1	0.03	-32.8	0.07							
26A14-1990-1	1	-7.0	0.03	-19.6	0.07							
26A14-1990-2	1	-9.3	0.03	-25.4	0.07							
26A14-1990-1†	2	-7.7	0.07	-27.2	0.04	-2.4	0.5	0.407	0.004	0.006	206	6
26A14-1990-2†	2	-7.8	0.57	-24.9	0.23	0.1	5.5	0.406	0.048	0.068	207	71
26A14-2110-1	1	-7.3	0.03	-27.6	0.07							
26A14-2110-2	1	-7.5	0.03	-32.2	0.07							
26A14-2110-1†	2	-8.5	0.29	-33.2	0.05	-7.6	3.2	0.399	0.0285	0.04	217	43
26A14-2110-2†	2	-9.7	0.16	-33.0	0.06	-8.1	1.1	0.405	0.010	0.015	208	14
26A14-2600-2	1	-7.0	0.03	-32.4	0.12							
26A14-2600-FG**	4	-13.4	0.05	-13.2	0.12	-12.1	0.6	0.711	0.007	0.014	19	2
3423-3320-2	1	-7.9	0.03	-26.0	0.07							
3814-3000-1	1	-8.6	0.03	-34.8	0.07							
3814-3000-2	1	-7.8	0.03	-33.3	0.07							
3814-3090-1	1	-9.6	0.03	-34.0	0.07							
3814-3090-2	1	-10.8	0.03	-25.5	0.07							
4127-4700-1	1	-6.7	0.03	-24.1	0.07							
4127-4700-2	1	-7.2	0.03	-16.2	0.07							
4127-5760-1	1	-5.6	0.03	-14.3	0.07							
4127-5760-2	1	-6.8	0.03	-25.7	0.07							
4127-5760-1†	2	-6.9	0.06	-22.6	0.04	-2.2	3.1	0.453	0.033	0.047	154	32
4127-5760-2†	2	-7.3	0.06	-25.9	0.02	-15.4	4.9	0.575	0.066	0.093	73	33
4127-6140-1	1	-7.3	0.03	-27.7	0.07							
4127-6140-2	1	-8.0	0.03	-28.6	0.07							
4127-6140**	2	-8.2	0.19	-27.3	0.43	-9.3	2.8	0.479	0.027	0.039	132	22

Sample identification reported as: well location, depth, and aliqout number (e.g. well# - sample depth - aliqout number).

† Clumped isotope data processed using separate aliquots.

** Clumped isotope data processed using combined aliquots.

'FG' Fault gouge observed in drilling log.

Table 2: Summary of stable and clumped isotope analyses. A continuation of the data is reported on next page.

Sample	# Replicates n	$\delta^{13}C$ (‰), (VPDB)	$\delta^{13}C$ (‰), Stnd error	$\delta^{18}O_{carb}$ (‰), (VPDB)	$\delta^{18}O_{carb}$ (‰), Stnd error	$\delta^{18}O_{H2O}$ (‰), (VSMOW)	$\delta^{18}O_{H2O}$ (‰), Stnd error	Δ_{47} (‰) ARF	Δ47 (‰) Stnd Error	Δ47 (‰) Stnd Dev	$T(\Delta_{47})$ (°C) Passey & Henkes	$T(\Delta_{47})$ Stnd error
4127-7690-1	1	-6.5	0.03	-23.3	0.12							
4127-7690-2	1	-6.0	0.03	-24.5	0.12							
5815-4450-1	1	-8.3	0.07	-24.1	0.01							
5815-4450-2	1	-8.2	0.03	-15.2	0.12							
5815-4450-2†	2	-7.8	0.05	-22.9	0.10	-3.1	5.5	0.459	0.059	0.083	148.578	56
5815-4930-1	1	-7.9	0.03	-27.4	0.07							
5815-4930-2	1	-5.1	0.03	-25.5	0.07							
5815-4930-2†	2	-7.3	0.06	-30.0	0.03	-6.3	3.7	0.417	0.036	0.051	192.647	45
5815-5360-2	1	-6.1	0.03	-29.0	0.12							
5815-5570-1	1	-8.3	0.03	-35.3	0.12							
5815-5570-2	1	-9.0	0.03	-34.2	0.12							
5815-5570**	2	-7.4	0.01	-30.4	0.03	-13.3	2.7	0.489	0.032	0.045	124.194	24
6122-3920-1	1	-7.0	0.03	-24.0	0.12							
6122-3920-2	1	-6.9	0.03	-23.9	0.12							
6122-4010-1	1	-6.8	0.03	-23.8	0.12							
6122-4010**	3	-7.2	0.01	-23.7	0.08	-4.6	1.1	0.467	0.011	0.019	141.62	10
6122-4980-1	1	-9.0	0.03	-30.4	0.12							
6122-4980-2	1	-6.7	0.03	-28.0	0.12							
6122-5510-2	1	-8.5	0.03	-35.8	0.12							
8622-3610-1	1	-7.0	0.03	-19.4	0.07							
8622-3610-2	1	-7.1	0.03	-21.3	0.07							
8622-4580-1	1	-10.1	0.03	-30.1	0.07							
8622-4580-2	1	-9.7	0.03	-29.7	0.07							
8911-2020-1	1	-7.2	0.03	-29.3	0.12							
8911-2020-2	1	-7.9	0.03	-30.3	0.12							
9115-4310-1	1	-8.2	0.03	-29.6	0.07							
9115-4310-2	1	-6.7	0.03	-26.3	0.07							
9115-4590-1	1	-7.6	0.03	-29.0	0.07							
9115-4590-2	1	-7.9	0.03	-32.0	0.07							
9115-4840-1	1	-8.6	0.03	-32.1	0.12							
9115-4840-2	1	-7.3	0.03	-29.4	0.12							
9115-6690-1	1	-6.8	0.03	-27.5	0.07							
9115-6690-2	1	-7.4	0.03	-20.0	0.07							
1-1723-1	1	-9.5	0.03	-32.4	0.06							
1-1723-2	1	-9.6	0.03	-29.7	0.06							
1-1770-1	1	-7.5	0.03	-31.4	0.06							
1-1770-2	1	-7.3	0.03	-32.8	0.06							
1-1960-1	1	-7.7	0.07	-31.8	0.01							
1-1960-2	1	-7.9	0.07	-32.1	0.01							
1-1960**	2	-7.9	0.01	-32.2	0.05	-11.3	2.7	0.445	0.028	0.040	161.724	28
2-720-FG**	2	-7.2	0.01	-29.6	0.01	-9.9	0.6	0.460	0.007	0.009	147.687	6
2-1583-1	1	-7.5	0.07	-33.5	0.01							
2-1583-2	1	-7.4	0.07	-33.4	0.01							
2-1583**	2	-7.4	0.06	-33.5	0.07	-13.3	0.7	0.453	0.006	0.009	154.053	6
2-2806-1	1	-9.2	0.07	-24.6	0.01							
2-2806-2	1	-9.2	0.07	-24.5	0.01							
2-2806†	2	-10.1	0.41	-25.6	0.03	-6.8	0.4	0.470	0.004	0.006	139.098	3
2-3456-2	1	-11.8	0.07	-25.2	0.01							
2-3456**	2	-11.7	0.01	-25.8	0.08	0.7	1.4	0.393	0.011	0.016	226.063	18
2-4607-1	1	-12.3	0.07	-24.5	0.01							
2-4607-2	1	-12.3	0.07	-22.5	0.01							

Sample identification reported as: well location, depth, and aliqout number (e.g. well# - sample depth - aliqout number).

† Clumped isotope data processed using separate aliquots.

** Clumped isotope data processed using combined aliquots.

'FG' Fault gouge observed in drilling log.

Table 3: Continued summary of stable and clumped isotope analyses.

3. RESULTS AND DISCUSSION

Stable and clumped isotope analyses are summarized in Table 1. The isotope results along with the results of the cold cathodoluminescence (CL) microscopy provide insight into geothermal fluid pathways and potential fluid sources.

3.1 Cold Cathodoluminescence (CL) Microscopy

Thin sections from the seven core samples were evaluated using transmitted and polarized light, as well as cold cathodoluminescence (CL) microscopy. Calcite from the seven core samples was found to occur at all depths as fracture fill that created a veneer on top of hydrothermal quartz. This layering indicates that the quartz-rich fluid was first to circulate through this system and is seen as the primary filler within the void spaces and fractures. The calcite within our samples shows reddish orange luminescence (Figure 2, bottom images). The thin sections from both cores exhibit this color luminescence, as well as calcite twinning. Luminescence patterns for the four samples from core DB-2 that were examined using CL microscopy did not indicate variations in the trace element composition of the calcite (Figure 2). However, two thin sections from the DB-1 core (depths 1723' and 1770') show distinct compositional changes in the form of CL banding (Figure 3). The observed banding was targeted and the separate bands were micro milled for further stable isotope analyses.

The banding most likely developed from fracture growth and marks the expansion of the fracture and calcite cement fill (e.g. Sippel and Glover, 1965; Morad *et al*, 2012). At a given location along a fracture, opening does not necessarily take place along the same plane during every open and fill event (David Budd, Professor of Geological Sciences, University of Colorado Boulder, written communication, 2014). For example, a fracture may open with calcite cements precipitating along the middle of the fracture. The next fracture growth may open a void along the outside wall of the fracture, which allows for calcite growth along the outside of the previous calcite deposit instead of growing inward. Overall, these findings show that the composition of the fluids within the reservoir has changed over time and that there were at least two compositional changes. Additionally, the banding reflects movement within the geothermal system and aperture growth along fractures.

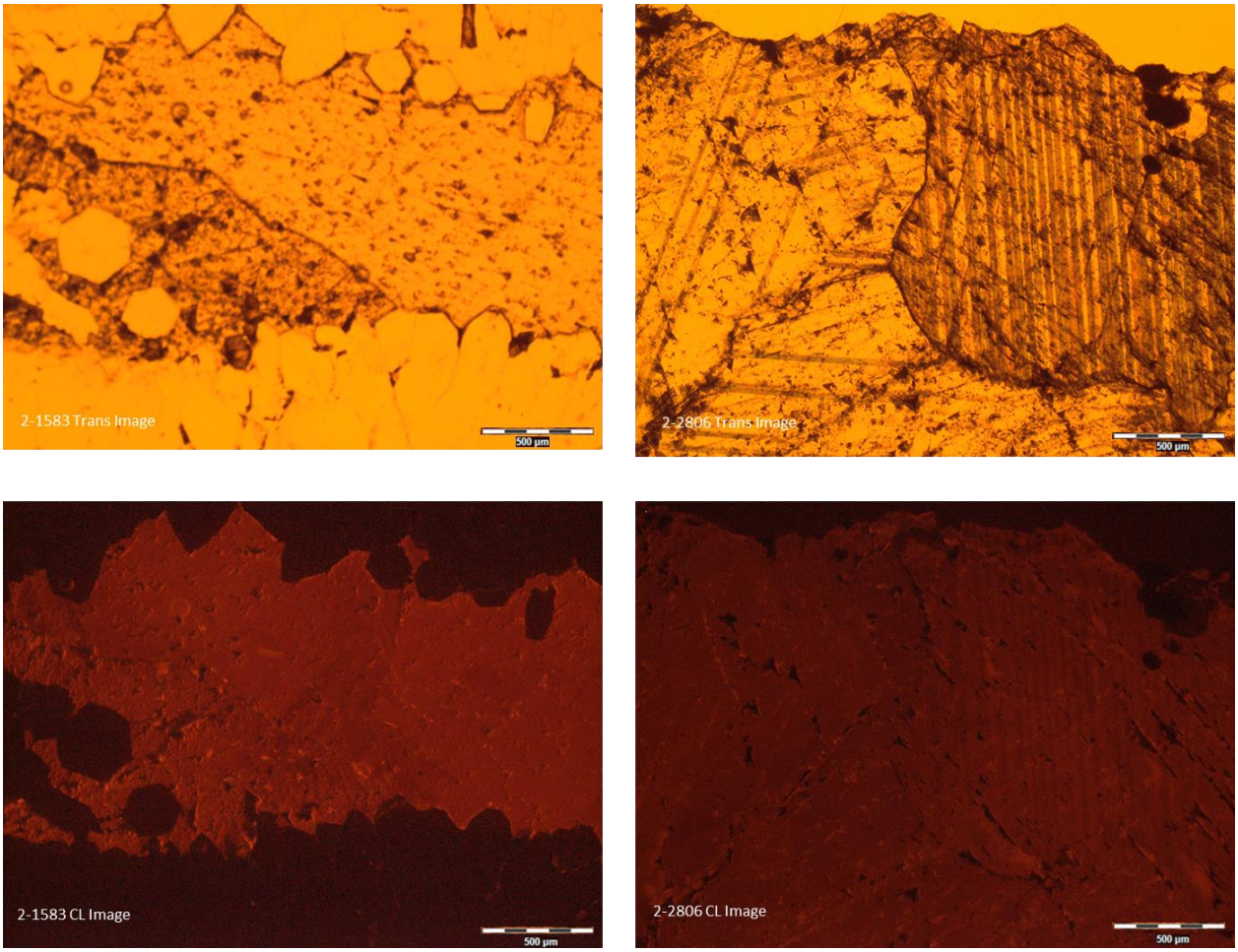

Figure 2: (Top) Transmitted light images of calcite taken from high-polished thin sections derived from core in well DB-2. (Bottom) Cathodoluminescence images taken at the same calcite location as the above transmitted light images. The CL coloring appears to be homogeneous throughout the calcite. The scale bar is 500 microns.

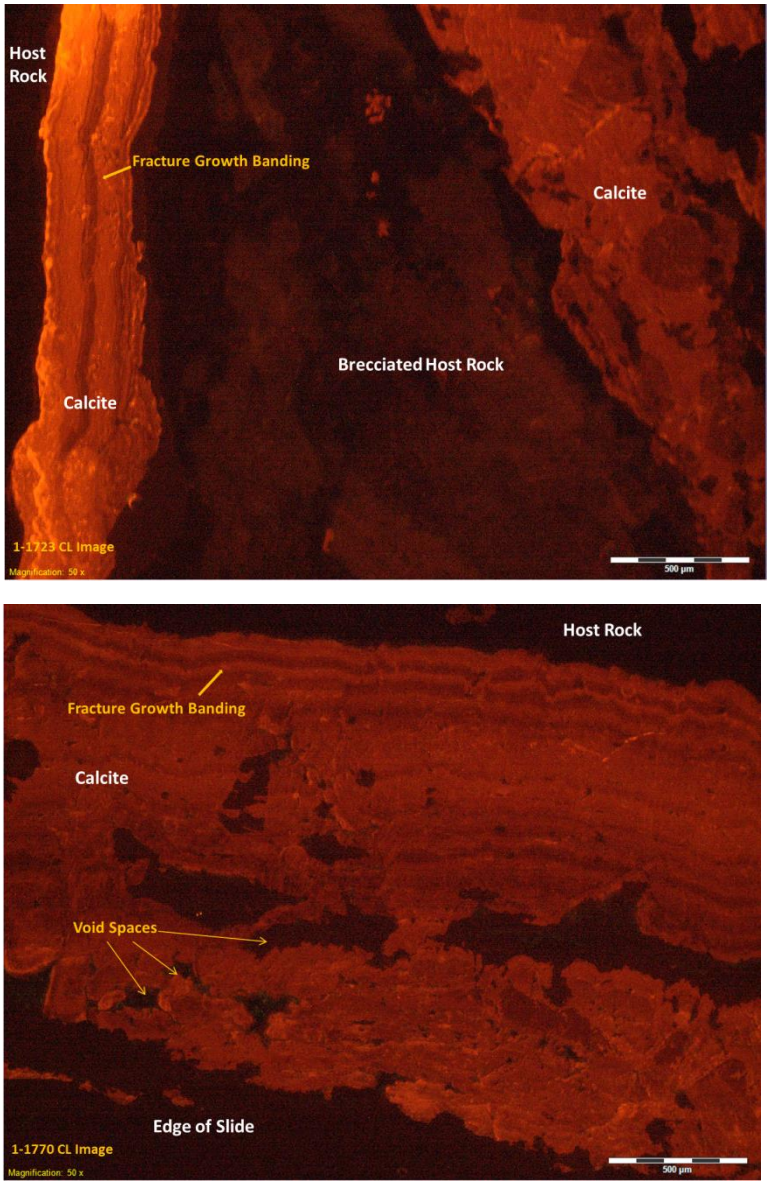

Figure 3: Cathodoluminescence images of calcite taken from high-polished thin sections derived from core in well DB-1. Light and dark banding is seen within the calcite core sample. The scale bar is 500 microns.

3.2 Stable Isotope Analysis

The $\delta^{18}O$ and $\delta^{13}C$ values of the carbonate samples establish compositional variations between each well using calcite samples derived from both drill cuttings and core. The seventy-two samples showed a wide range of $\delta^{18}O_{Carbonate}$ values from -19.4 ‰ to -35.8‰ (VPDB), which had standard errors no greater than +/- 0.1‰ (Table 1). The $\delta^{13}C$ stable isotopic values for the seventy-two samples varied from -5.1‰ to -12.3‰, +/- 0.1‰ (VPDB) (Table 1). In some cases, the two separate samples of calcite that were analyzed from the same well and depth interval showed large variations in carbonate $\delta^{18}O$ and $\delta^{13}C$ values. In addition to these seventy-two carbonate samples for which conventional $\delta^{18}O$ and $\delta^{13}C$ values are reported, the carbonate $\delta^{18}O$ and $\delta^{13}C$ values measured concurrently with clumped isotope analysis of nineteen additional samples also reflect this broad range of values. The $\delta^{18}O_{Carbonate}$ values for the subset targeted for clumped isotope analysis ranged from -13.2‰ to -33.5‰ (VPDB) with a measured standard error generally less than +/- 0.1‰ (Table 1). Additionally, the subset of nineteen samples that were analyzed for clumped isotope thermometry had similar ranges of $\delta^{13}C$ values (-6.7‰ to -13.4‰), with standard errors generally less than +/- 0.1‰ (VPDB) (Table 1).

The range of values found in the calcite $\delta^{18}O$ and $\delta^{13}C$ values demonstrates the variability of the fluids through the system, which is recorded in the precipitated calcite cements. Some wells within the geothermal field reflected homogenous results throughout the well depths, while other sampled wells were highly variable (Figure 4). An example of this fluid variation is from one of the micro milled samples (DB-1 at depth interval 1,723 feet) extracted from the growth banding observed in the CL images. This sample recorded a calcite $\delta^{18}O$ value of -32.4‰ +/- 0.1‰ (VPDB) for the light colored band and -29.7‰ +/- 0.1‰ (VPDB) for the darker band, which

reflects a ~ 3‰ difference. In contrast, the banding seen in the other core sample (DB-1 at depth interval 1,770 feet) showed a calcite $\delta^{18}O$ value of -32.8‰ +/- 0.1‰ (VPDB) for the light colored band, and -31.4‰ +/- 0.1‰ (VPDB) for the darker band, which shows very little variation. The $\delta^{13}C$ results for the banding at each well depth for the two micro milled core samples were virtually the same (Figure 5) (Table 1).

Some calcite $\delta^{18}O$ values found throughout the sampled wells in the geothermal field were sometimes in agreement with values from other wells, which may suggest connectivity between two or more wells. However, variations in calcite $\delta^{18}O$ and $\delta^{13}C$ values can be from either changes in temperatures, fluid composition, or both (Zheng and Hoefs, 1993). Because of our broad range of calcite $\delta^{18}O$ values, further Δ_{47} analysis is needed to aid in identifying whether temperature is influencing the variable behavior.

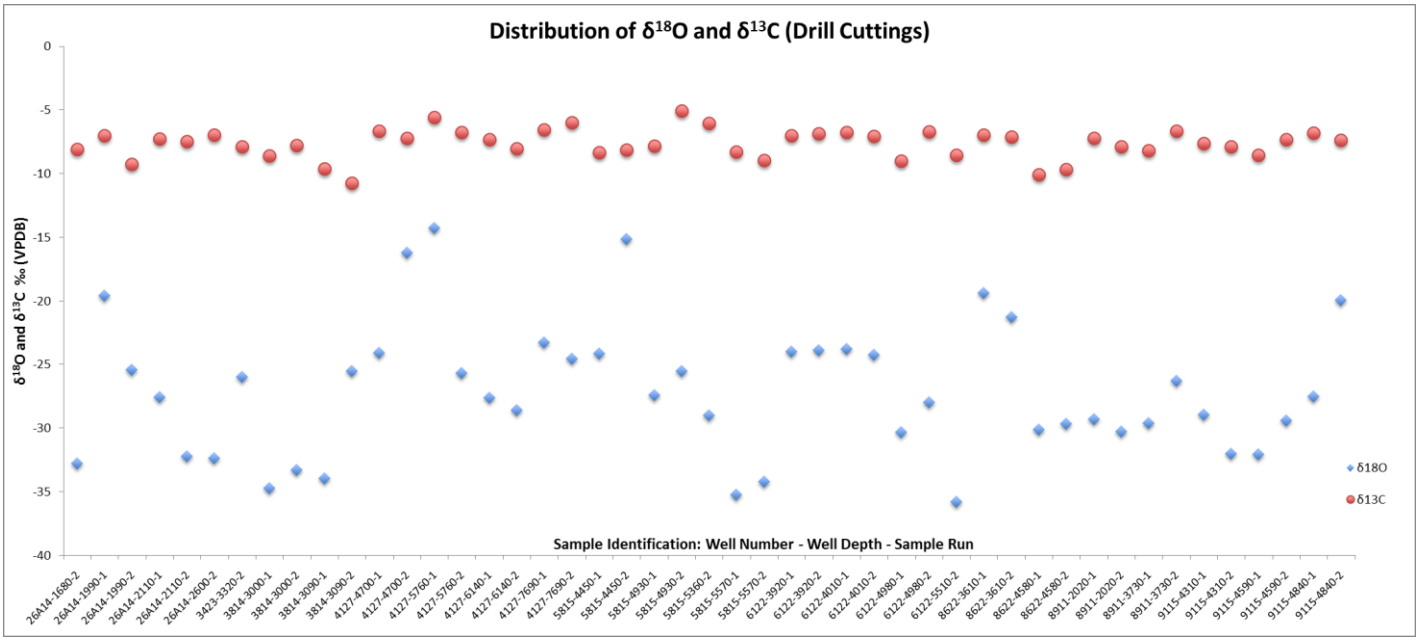

Figure 4: Results from the stable isotope analysis given for each sampled well within the Blue Mountain geothermal field. These results are derived from drill cuttings. Large variations can be seen between the wells; whereas, some wells reflect homogeneity within the data.

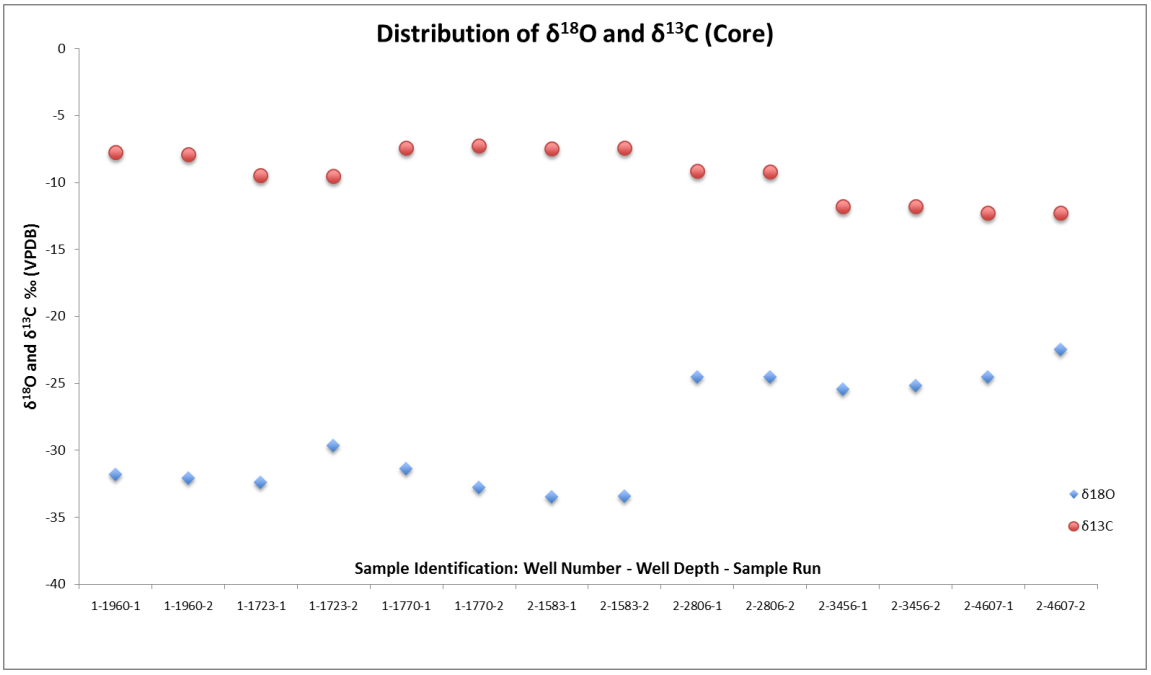

Figure 5: Results from the stable isotope analysis given for each sampled well within the Blue Mountain geothermal field. These results are derived from the core. CL imaging generally showed one generation of calcite except in core DB-1, which can be seen as slight peaks in the graph (samples 1-1723 and 1-1770). Otherwise, very little variation is observed, which reflects homogeneity within the precipitated calcite.

3.3 Clumped Isotope (Δ_{47}) Analysis

The subset of samples from both drill cuttings and core was chosen for clumped isotope thermometry to further investigate the cause of the variations seen in the conventional calcite $\delta^{18}O$ and $\delta^{13}C$ values. The Δ_{47} values from our clumped isotope thermometry analyses of the seventeen homogeneous calcite cement samples range from 0.39‰ to 0.71‰ with errors less than +/- 0.1‰ (ARF). These values correspond to calcite precipitation temperatures of ~226°C to ~19°C calculated using the equation of Passey and Henkes (2012), with average temperature uncertainties generally less than 40°C. Most calcites we analyzed precipitated at temperatures of ~124°C to ~226°C (Table 1). However, two samples taken from wells 26A-14 and 41-27 at respective depths of 2,600ft and 5,760ft record much cooler temperature values of 19°C and 73°C respectively, which were confirmed by replicate analyses of the samples (Table 1). The $\delta^{18}O_{H2O}$ values calculated from the measured temperatures and calcite $\delta^{18}O$ values show a range of -15‰ to 0.7‰ (VSMOW).

Comparison of paleofluid temperatures and $\delta^{18}O_{carbonate}$ values derived from calcite cements from the same well and well depth did not show any significant trends (Figure 6). Because of the consistency of temperature with varying $\delta^{18}O_{Carbonate}$ (VPDB) values, we may be able to consider the connectedness between other wells within the geothermal field based on their similar conventional calcite $\delta^{18}O$ values. Additionally, correspondence of paleofluid temperatures and $\delta^{18}O_{H2O}$ values derived from calcite cements from different wells may also suggest hydraulic connectedness between those wells at the time of cement precipitation. If temperatures and $\delta^{18}O_{H2O}$ values show agreement with other wells throughout the field, then this would also imply connectivity.

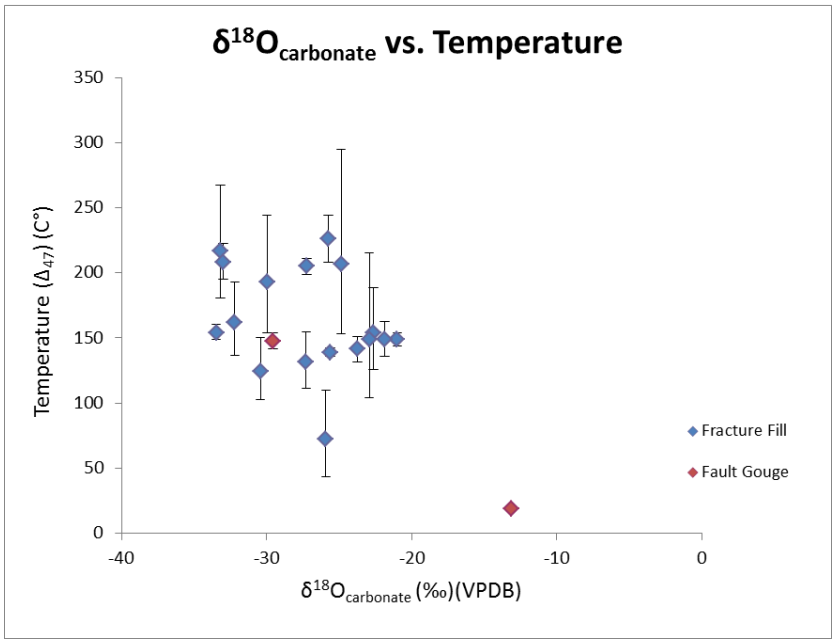

Figure 6: Graph of paleofluid temperature Δ_{47} versus the $\delta^{18}O_{Carbonate}$ (VPDB). Temperature does not appear to necessarily influence the measured variations of the calcite $\delta^{18}O$ values.

We can interpret the paleofluid temperatures inferred from clumped isotope analysis in the context of structural position within the geothermal field. Paleofluid temperatures within the geothermal field at the time of calcite precipitation for most of our samples are similar to current reservoir temperatures, which are approximately 167°C, but two calcite cements recorded significantly cooler Δ_{47} values similar to earth-surface temperatures. One of the cooler precipitation temperatures of 19°C at 2,600 feet depth was derived from calcite in fault gouge recorded in drill logs (26A14-2600-FG). This cool 2,600 foot-depth sample is capped above by two measured Δ_{47} temperatures of >200°C at depths of 1,990 and 2,110 feet in the same well. This cool temperature could indicate a meteoric recharge path where a fault within the geothermal field funneled cooler surface waters down into the reservoir. The other fault related sample (DB2-720'); however, is within the temperature range of other "hot" sampled fracture fill cements. Additionally, a non-fault gouge sample taken at 5,280 feet showed a cooler-than-ambient precipitation temperature of 73°C, which likely also points to a fault-controlled meteoric fluid pathway. Except for the two anomalous temperature data points, the temperature within the reservoir stays close to a paleotemperature of approximately 150°C with several wells peaking at above 200°C. The consistency of the reservoir temperatures seen throughout the other seventeen samples is interpreted as related to convective cycling of fluids through the system.

Other interesting observations within this dataset are the depth-dependent relationships of $\delta^{18}O_{H2O}$, $\delta^{13}C_{carbonate}$, and Temperature (Δ_{47}) (Figure 7). There are two depth intervals (2,000ft to 3,500ft and 5,500ft to 6,000ft) that are characterized by an apparent shift in both the stable isotope values and in temperature. One of the isotopic and temperature shifts (well 26A14-2600-FG) within this depth interval is related to a fault, and other excursions from the trend may reflect additional faults within the field that are influencing fluid migration.

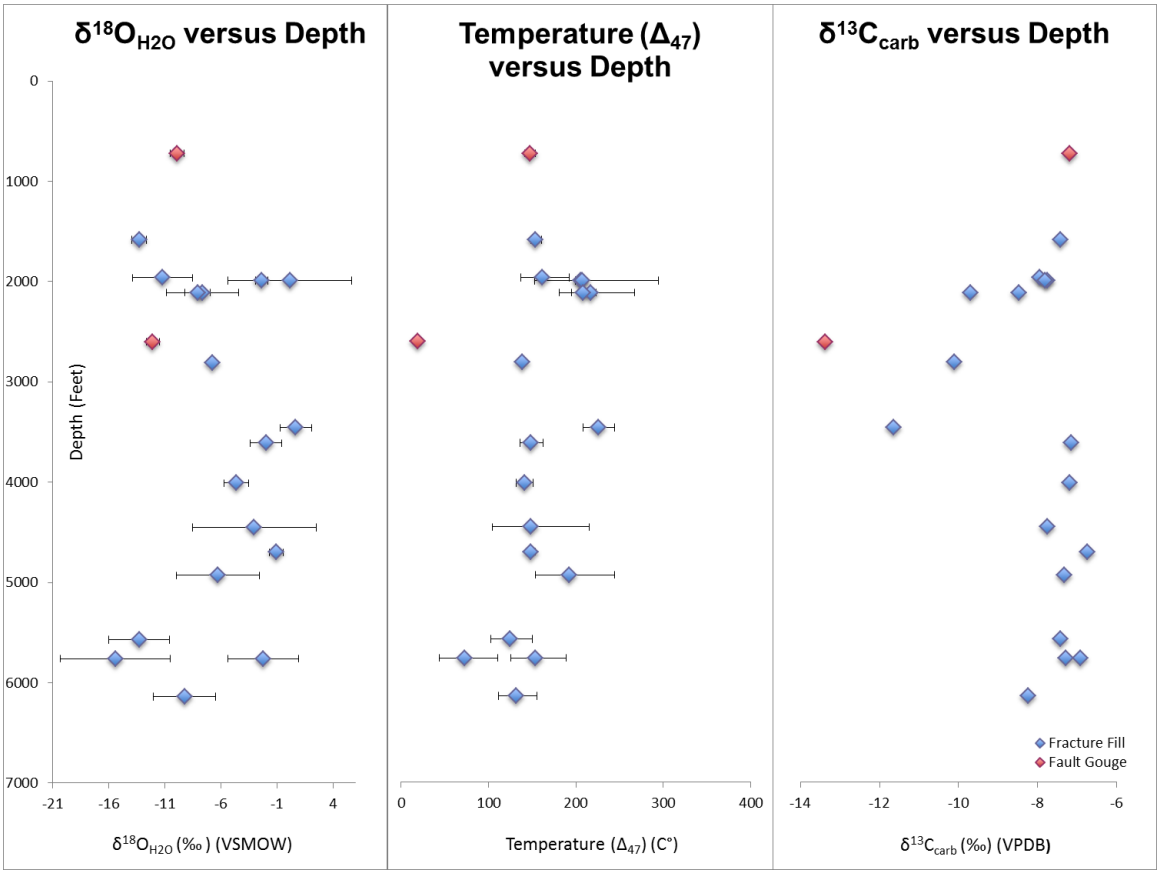

Figure 7: Graph of $\delta^{18}O_{H2O}$, $\delta^{13}C_{Carb}$, and temperature relationship with depth. There are two depth intervals at 2,000 - 3,500 feet and 5,500 feet - 6,000 feet that show excursions from each dataset trend.

4. CONCLUSIONS

This pilot project intended to assess the utility of a new combination of stable isotope techniques for the purpose of determining past fracture connectivity within a geothermal reservoir. We find that both calcite cements from cuttings and core samples can yield useful isotopic data for characterizing paleofluids and past fracture connectivity in a geothermal field. However, our results show the importance of evaluating cement homogeneity using conventional $\delta^{13}C$, $\delta^{18}O$ and CL observations prior to clumped isotope analysis to ensure meaningful results. From our CL analysis, we are also able to confirm that the fluids within the geothermal system have changed in composition throughout the field's lifespan, and that the size of the apertures of the fractures moving the fluids has also changed. The samples with cooler-than-modern ambient Δ_{47} precipitation temperatures may indicate that meteoric fluids were funneled down into this system through conduits such as faults. The measured Δ_{47} temperatures also show that average reservoir temperature has not changed much since precipitation of our calcite cements. Moreover, correspondence of the stable isotope temperature and $\delta^{18}O_{H2O}$ values constrained by clumped isotope thermometry of calcite for different wells may show connectedness among wells within the geothermal field.

REFERENCES

Bergman, S. C., Huntington, K. W., Crider, J. G.: Tracing Paleofluid Sources using Clumped Isotope Thermometry of Diagenetic Cements along the Moab Fault, Utah. *American Journal of Science*, **313:5**, (2013), 490-515.

Boggs, S., Krinsley, D.: Application of Cathodoluminescence Imaging to the Study of Sedimentary Rocks. *Cambridge University Press*, (2006).

Bottomley, D. J., Veizer, J.: The Nature of Groundwater Flow in Fractured Rock: Evidence from the Isotopic and Chemical Evolution of Recrystallized Fracture Calcites from the Canadian Precambrian Shield. *Geochimica et Cosmochimica acta*, **56:1**, (1992), 369-388.

Bruel, D.: Impact of Induced Thermal Stresses during Circulation Tests in an Engineered Fractured Geothermal Reservoir: Example of the Soultz-Sous-Forets European Hot Fractured Rock Geothermal Project, Rhine Graben, France. *Oil & Gas Science and Technology*, **57:5**, (2002), 459-470.

Clark, I. D., and Fritz, P.: Environmental Isotopes in Hydrogeology. *CRC Press*, (1997).

De Abajo, F. G.: Optical Excitations in Electron Microscopy. *Reviews of Modern Physics*, **82:1**, (2010), 209.

Dennis, K. J., Affek, H. P., Passey, B. H., Schrag, D. P., Eiler, J. M.: Defining an Absolute Reference Frame for 'Clumped'Isotope Studies of CO_2. *Geochimica et Cosmochimica Acta*, **75:22**, (2011), 7117-7131.

Eiler, J.M.: "Clumped-Isotope" Geochemistry – The Study of Naturally-Occurring, Multiply-Substituted Isotopologues. *Earth and Planetary Science Letters*, **262:3-4**, (2007), 309-327.

Faulds, J.E., Melosh, G.: A Preliminary Structural Model for the Blue Mountain Geothermal Field, Humboldt County, Nevada. *GRC Transactions*, **32**, (2008), 273-278.

Friedman, I., Harris, J. M., Smith, G. I., Johnson, C. A.: Stable Isotope Composition of Waters in the Great Basin, United States 1. Air-mass Trajectories. *Journal of Geophysical Research: Atmospheres*, **107:D19**, (2002), ACL-14.

Ghosh, P., Adkins, J., Affek, H., Balta, B., Guo, W., Schauble, E. A., Eiler, J. M.: ^{13}C-^{18}O Bonds in Carbonate Minerals: A New Kind of Paleothermometer. *Geochimica et Cosmochimica Acta*, **70:6**, (2006), 1439-1456.

Haas, J., Demény, A., Hips, K., Vennemann, T. W.: Carbon Isotope Excursions and Microfacies Changes in Marine Permian–Triassic Boundary Sections in Hungary. *Paleogeography, Paleoclimatology, Paleoecology*. **237:2**, (2006), 160-181.

Henkes, G. A., Passey, B. H., Wanamaker Jr, A. D., Grossman, E. L., Ambrose Jr, W. G., Carroll, M. L.: Carbonate Clumped Isotope Compositions of modern Marine Mollusk and Brachiopod Shells. *Geochimica et Cosmochimica Acta*, **106**, (2013), 307-325.

Horne, R. N., Rodriguez, F.: Dispersion in Tracer Flow in Fractured Geothermal Systems. *Geophysical Research Letters*, **10:4**, (1983), 289-292.

Huntington, K. W., Eiler, J. M., Affek, H. P., Guo, W., Bonifacie, M., Yeung, L.Y., Thiagarajan, N., Passey, B., Tripati, A., Daeron, M., Came, R.: Methods and Limitations of 'Clumped'CO_2 Isotope (Δ_{47}) Analysis by Gas-Source Isotope Ratio Mass Spectrometry. *Journal of Mass Spectrometry*, **44:9**, (2009), 1318-1329.

Kim, S. T., O'Neil, J. R.: Equilibrium and Nonequilibrium Oxygen Isotope Effects in Synthetic Carbonates. *Geochimica et Cosmochimica Acta*, **61:16**, (1997), 3461-3475.

Lowell, R. P., Van Cappellen, P., Germanovich, L. N.: Silica Precipitation in Fractures and the Evolution of Permeability in Hydrothermal Upflow Zones. *Science*, **260:5105**, (1993), 192-194.

Machel, H. G.: Cathodoluminescence in Calcite and Dolomite and its Chemical Interpretation. *Geoscience Canada*, **12:4**, (1985), 139-147.

Meinert, L. D.: Skarns and Skarn Deposits. *Geoscience Canada*, Vol. **19:4**, (1992).

Morad S., Ketzer, M., deRos, L.F.: Linking Diagenesis to Sequence Stratigraphy. John Wiley & Sons, West Sussex, UK (2012).

Passey, B. H., Henkes, G. A.: Carbonate Clumped Isotope Bond Reordering and Geospeedometry. *Earth and Planetary Science Letters*, **351**, (2012), 223-236.

Pirajno, F.: Hydrothermal processes and mineral systems. Springer (2008).

Schauble, et al.: Preferential Formation of ^{13}C-^{18}O Bonds in Carbonate Minerals, Estimated using First-Principles Lattice Dynamics. *Geochimica et Cosmochimica Acta*, **70:10**, (2006), 2510-2529.

Sheridan, J., Kovac, K., Rose, P., Barton, C., McCulloch, J., Berard, B., Moore, J.M., Petty, S., Spielman, P.: In Situ Stress, Fracture and Fluid Flow Analysis—East Flank of the Coso Geothermal Field. *Proceedings*, 28th Workshop on Geothermal Reservoir Engineering, Stanford University, Stanford, CA (2003).

Sippel, R. F., Glover, E. D.: Structures in Carbonate Rocks made Visible by Luminescence Petrography. *Science*, **150:3701**, (1965), 1283-1287.

Slater, C., Preston, T., Weaver, L. T.: Stable Isotopes and the International System of Units. *Rapid Communications in Mass Spectrometry*, **15:15**, (2001), 1270-1273.

Swanson, E. M., Wernicke, B. P., Eiler, J. M., Losh, S.: Temperatures and Fluids on Faults based on Carbonate Clumped–Isotope Thermometry. *American Journal of Science*, **312:1**, (2012), 1-21.

Wyld, S. J.: Structural Evolution of a Mesozoic Backarc Fold-and-Thrust Belt in the US Cordillera: New Evidence from Northern Nevada. *Geological Society of America Bulletin*, **114:11**, (2002), 1452-1468.

Yasuhara, H., Polak, A., Mitani, Y., Grader, A. S., Halleck, P. M., Elsworth, D.: Evolution of Fracture Permeability through Fluid–Rock Reaction under Hydrothermal Conditions. *Earth and Planetary Science Letters*, **244:1**, (2006), 186-200.

Zheng, Y. F., Hoefs, J.: Carbon and Oxygen Isotopic Covariations in Hydrothermal Calcites, *Mineralium Deposita*, **28:2**, (1993), 79-89.